Scaling of Star Polymers with 1−80 Arms

Hsiao-Ping Hsu,* Walter Nadler, and Peter Grassberger

John-von-Neumann Institute for Computing, Forschungszentrum Jülich, D-52425 Jülich, Germany

Received October 22, 2003; Revised Manuscript Received March 15, 2004

ABSTRACT: We present large statistics simulations of 3-dimensional star polymers with up to $f = 80$ arms and with up to 4000 monomers per arm for small values of f. They were done for the Domb−Joyce model on the simple cubic lattice. This is a model with soft core exclusion which allows multiple occupancy of sites but punishes each same-site pair of monomers with a Boltzmann factor $v < 1$. We use this to allow all arms to be attached at the central site, and we use the "magic" value $v = 0.6$ to minimize corrections to scaling. The simulations are made with a very efficient chain growth algorithm with resampling, PERM, modified to allow simultaneous growth of all arms. This allows us to measure not only the swelling (as observed from the center-to-end distances) but also the partition sum. The latter gives very precise estimates of the critical exponents γ_f. For completeness we made also extensive simulations of linear (unbranched) polymers which give the best estimates for the exponent γ.

1. Introduction

Star polymers are of interest both for their technical applications, ranging from lubricant additives to paints,[1,2] and for the theoretical challenge which they represent. Polymer theory in general is one of the prime fields where renormalization group theory can be used and compared in detail with real experiments.[3,4] The simplest nontrivial objects in this respect are the partition sum and the rms end-to-end distance of a single long flexible linear (unbranched) polymer with N monomers in a good solvent, which scale as

$$Z_N \sim \mu^{-N} N^{\gamma-1} \tag{1}$$

and

$$R_N^2 \approx A_1 N^{2\nu} \tag{2}$$

Star polymers, i.e., f such chains linked together at a single point, are some of the simplest examples of polymers with nontrivial topology. As shown by Duplantier,[5] all such polymer networks are characterized by equations similar to eqs 1 and 2, with the critical fugacity μ and the critical exponent ν being the same for all topologies, but with γ being universal only within each topology. For star polymers composed of f arms of length N each, one has in particular

$$Z_{N,f} \sim \mu^{-fN} N^{\gamma_f-1} \tag{3}$$

and

$$R_{N,f}^2 \approx A_f N^{2\nu} \tag{4}$$

where $R_{N,f}$ is the rms Euclidean center-to-end distance.

The behavior of γ_f and of the swelling factor A_f are of central interest, for both finite f and for $f \to \infty$. In two dimensions, γ_f can be calculated exactly using conformal invariance,[5] but no exact results are known for $d = 3$. Renormalization group methods give ϵ expansions up to third power in $\epsilon = 4 - d$,[6] but these are nonconvergent power series and have to be resummed before being applicable in $d = 3$. The results are debated, in particular for large values of f.[7] For the swelling factor the situation is similarly unclear. Phenomenologists tend to compare with predictions based on Gaussian (i.e., free) chains[8] or on heuristic assumptions.[9,10] There exist several renormalization group calculations, but those not based heavily on simulation data[11,12] seem to describe some of the data rather poorly, and Monte Carlo simulations are needed to fix free parameters in such theories.[13,14]

In view of this, Monte Carlo[15−20] and molecular dynamics[21,22] simulations have played a major role in the efforts to understand the behavior of star polymers. Molecular dynamics simulations[22] have indeed been used to study very large stars, with up to 80 arms of length $N = 100$ each, but it is not clear whether these simulations have really reached equilibrium. Moreover, both molecular dynamics and Monte Carlo methods with fixed chain lengths (including the pivot algorithm[14,20]) cannot measure the partition sum and thus give no information on γ_f. For the latter one has to use chain growth methods.[15−17,19,20,23] Unfortunately, with the methods used so far it has not been possible to go beyond 24 arms,[17] and even these were too short and the data were too noisy to provide a clear-cut picture of the asymptotic behavior.

We decided therefore to perform simulations with several improvements which allow us to reach much larger systems and much higher accuracy. To obtain a good estimate for μ and for the critical exponents of unbranched polymers, we also made extensive simulations of linear chains. The model and the method of simulation are described in the next section. Results are given in section 3, while we end with a discussion in section 4.

2. Model and Method

Let us first describe in detail our model. For efficiency, and since we are only interested in scaling behavior, we use a lattice model. Indeed, we use the simplest version, the simple cubic lattice. But instead of simulating self-avoiding walks as in previous works, we simulate the Domb−Joyce model[24] at its "magic" interaction strength $v = v^*$. In the Domb−Joyce model polymers are described by lattice walks where monomers sit at sites and are connected by bonds of length 1. Multiple

10.1021/ma0355958 CCC: $27.50
Published on Web 05/14/2004

visits to the same site are allowed, but for any pair of monomers occupying the same site one has a repulsive energy $\epsilon > 0$, giving rise to a Boltzmann factor $v = \exp(-\beta\epsilon) < 1$. The partition sum of a linear chain molecule of $N + 1$ monomers is thus a sum over all walks of N steps, each weighted with v^m, where m is the total number of pairs occupying the same site, $m = \sum_{i<j} \delta_{x_i,x_j}$. For star polymers we studied in the present work two variants. In both variants arms of N monomers are attached to a central site. In the first variant, the central site is singly occupied. In the second, it is occupied by f monomers, one for each arm. We studied both variants in order to verify that results were independent of this detail, and we include in our final error estimates the uncertainty it entails.

Using the Domb−Joyce model has two main advantages. First of all, it allows us to attach a large number of arms to a pointlike center. In the present work, we go up to $f = 80$.[25] Previously, authors had used extended cores. Although these cores were much smaller than the radii of the polymers themselves and should thus not destroy the asymptotic scaling, they do introduce a finite length scale and present therefore corrections to scaling terms which complicate the analysis.

More important is that there is one special ("magic") value of v, called v^* in the following, where corrections to scaling are minimal and where asymptotic scaling laws are reached fastest. For single chains it has been estimated[26,27] as $v^* \approx 0.6$ with rather small error bars, and we shall in the following assume this value to be exact. In the renormalization group language, the flow of the effective Hamiltonian to its fixed point in the stable manifold of the latter contains one direction of slowest approach. For a generic starting point there is a nonzero component in this direction, which then determines the leading correction to scaling. If one starts however with the flow such that this component is absent, the approach to scaling is governed by the next-to-leading correction term and is much faster. A similar observation has been made also for off-lattice bead−rod models with fixed bond length, where the leading corrections to scaling are absent for a certain "magic" ratio between bead size and rod length.[28−30]

Since the value of v^* should depend only on the internal structure of the chains, for star polymers it should be independent of the number of arms. For the bead−rod model this was carefully verified in ref 14. We thus simulated only with $v = v^*$.

For our simulations we used the pruned-enriched Rosenbluth method (PERM).[31] This is a biased chain growth algorithm, similar to the Rosenbluth−Rosenbluth[32] method. In the latter, the bias induced by avoiding double occupancy is compensated by a weight factor which is basically of entropic origin. In the present case, we have both a bias compensating factor and a Boltzmann factor, the product of which tends to fluctuate wildly if there is no perfect importance sampling. These fluctuations are suppressed in PERM by pruning low-weight configurations and cloning those with high weight. Indeed, any bias can be employed in PERM, as long as it can be compensated by a weight factor. In previous simulations of diluted polymers we use a Markov approximation called Markovian anticipation.[33−35] In the present case we did not expect this to be very useful because the main interactions are not within one arm but between different arms. Thus, we used instead a very simple bias where each arm tends to grow preferentially outward (except for the simulations for $f = 1$ where we used of course Markovian anticipation). The strength of this bias was adjusted by trial and error. It decreased with the length of the arm and increased with f. Details will not be given since they are not very important, and working without this bias would have increased the errors by only a factor ≈2, in general.

A final comment is that it is easy to modify the basic PERM algorithm given for example in the appendix of ref 31 such that all f arms are grown simultaneously.[36] This is done by having f growth sites x_1, ..., x_f. Chain growth is made in PERM by calling recursively a subroutine for each monomer addition. For multiarm growth, we add an integer $k \in [1, ..., f]$ to the argument list of this subroutine, such that a subroutine called itself with argument k calls the next subroutine with $(k \bmod f) + 1$. In this way a monomer is added to each arm before the next round of monomers is added. Compared to a scheme where one arm is grown entirely before the next arm is started, the main advantage is that each chain grows in the field of all the others and is thus, by the population control (pruning/cloning), guided to grow into the correct outward direction. If chains were grown one after the other, this bias would be absent for the first chains which then would grow into "wrong" directions, resulting in very low-weight configurations.

3. Results

3.1. Partition Sums and γ-Exponents. One of the outstanding features of chain growth methods such as PERM is that they give estimates for the partition sum. Indeed, these estimates are a basic part of the simulations since the population control is based on these estimates.

According to eq 3, we expect $Z_{N,f}\mu^{fN}$ to approach a power law $const\ N^{\gamma_f - 1}$ at large N. One precise way to estimate γ_f is to subtract a term $a_f \ln N$ from $\ln(Z_{N,f}\mu^{fN})$ and adjust the constant a_f such that the difference gives a flat curve for large N, when plotted against $\ln N$. This then gives $\gamma_f = 1 + a_f$. Alternatively, we could plot $\ln Z_{N,f} - \ln Z_{fN,1} - a_f' \ln N$ against $\ln N$, in which case a flat curve is obtained when $a' = \gamma_f - \gamma$. We prefer both methods over a least-squares fit, say, since they allow directly to check visually for the presence of corrections to scaling. If such corrections seem needed, one can subtract them and obtain in this way the most reliable and precise estimates of γ_f —remembering of course that estimating a critical index involves an extrapolation and is thus ill-posed, giving at best subjective error estimates.

For either method we need precise estimates of the partition sum of linear chains. We thus performed first extensive simulations of linear ($f = 1$) Domb−Joyce chains, creating altogether $\approx 4 \times 10^8$ chains of length $N = 8000$. In Figure 1, we plot effective exponents obtained from triple ratios[26] $Z^x_{aN} Z^y_{bN}/Z_N$. Here a and b are chosen such as to minimize statistical and systematic errors,[26] and powers x and y are fixed such that μ and the overall normalization drop out. With $a = 1/3$ and $b = 5$ we have

$$\gamma_{\text{eff}}(N) = 1 + \frac{7 \ln Z_N - 6 \ln Z_{N/3} - \ln Z_{5N}}{\ln(3^6/5)} \qquad (5)$$

which is plotted against $1/N^{0.96}$. The fact that we find

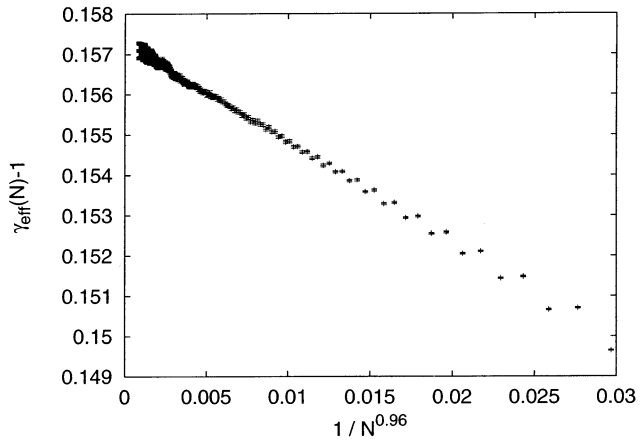

Figure 1. Effective exponents $\gamma_{eff}(N)$ for linear ($f = 1$) "magical" Domb−Joyce polymers against $1/N^{0.96}$.

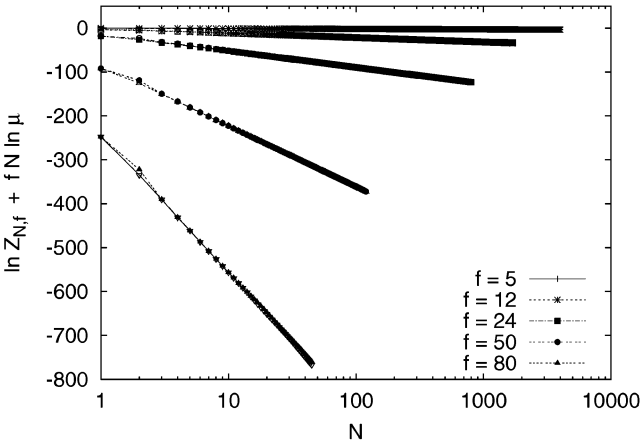

Figure 2. Logarithms of the partition functions $Z_{N,f}$ multiplied by $\mu^{f\,N}$. For each pair of close-by lines, the upper refers to singly occupied centers, while the lower one has f monomers located at the center.

essentially a straight line (apart from odd/even oscillations due to the special structure of the cubic lattice) indicates that the leading correction to scaling exponent is $\Delta \approx 0.96$, which is much larger than the value $\Delta \approx {}^1/_2$ for generic self-avoiding walks, indicating that $\nu = 0.6$ is indeed close to the magic value. Our estimate is therefore

$$\gamma = \lim_{N\to\infty} \gamma_{\mathrm{eff}}(N) = 1.1573 \pm 0.0002 \qquad (6)$$

This is in good agreement with the best previous estimates[26,37] but more precise. Using this estimate, we obtain then

$$\mu = 0.18812145 \pm 0.00000003 \qquad (7)$$

After having obtained a precise estimate for μ, we can now discuss the results for stars. Results for a few selected values of f are shown in Figure 2. We plot there $\ln Z_{N,f} + f\,N \ln \mu$ for both variants, i.e., the center singly occupied or f times occupied. The latter gives smaller values of $Z_{N,f}$, but the difference is visible only for $N = 2$. For larger N both agree, except for $f = 80$ and large values of N where our sampling algorithm starts to break down.

For a precise estimate of γ_f we of course did not use plots like Figure 2, but we subtracted $(\gamma_f - 1) \ln N$ as explained above. Then we see (Figure 3) that there are nonnegligible corrections to scaling, but our arms are

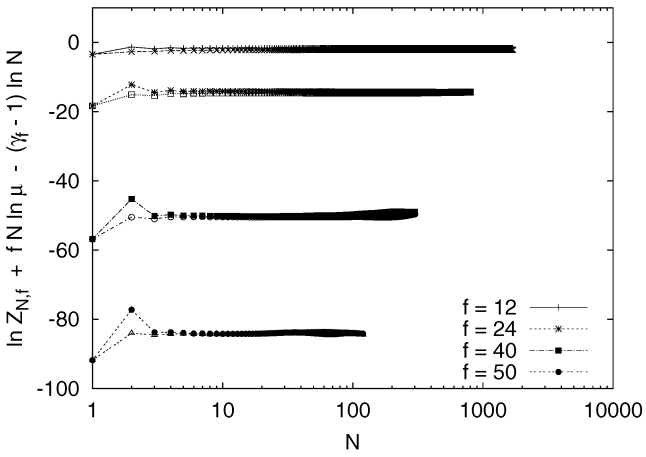

Figure 3. Logarithms of the partition functions $Z_{N,f}$ multiplied by $\mu^{f\,N}$, plus $(1 - \gamma_f) \ln N$. For each pair of close-by lines, the upper refers again to singly occupied centers, while the lower one has f monomers located at the center.

long enough so that our estimates of γ_f are not affected by them. Our final results, obtained by averaging over both variants of the model, are shown in Table 1 and in Figure 4. In Table 1 we also give additional information such as the arm lengths and the total statistics. We also list previous estimates for comparison. We see reasonable agreement in general, although those previous estimates which were quoted with error bars[16] are off by many standard deviations. We should add that the simulations in ref 16 involved much shorter chains and lower statistics.

Previous theoretical predictions of γ_f used $\epsilon = 4 - d$-expansions[6,7] and the cone approximation.[38,39] The latter assumes that each branch is confined to a cone of space angle $4\pi/f$ and gives

$$\gamma_f - 1 \sim -f^{3/2} \qquad (8)$$

As seen from Figure 4, this is not too far off, but it definitely does not provide a quantitative fit to our data. The best fit with a power law $\gamma_f - 1 \sim -(f - 1.5)^z$ would be obtained with $z \approx 1.68$, but we do not claim that this exponent has any deeper significance.

In contrast to the cone approximation which is basically heuristic and cannot be improved systematically, ϵ-expansions have a firm theoretical basis. But the expansion itself is at best asymptotic, and each term gives a contribution to γ_f which is polynomial in f. Thus, it cannot be used without resummation. Such resummations have not yet been attempted for $f \to \infty$. For small f, results are given in refs 6 and 7 and are listed in Table 1. They are in the correct order of magnitude, but their precision is not sufficient to draw any firm conclusion beyond the fact that the resummed ϵ-expansion is obviously not in conflict with the Monte Carlo data.

3.2. Coil Sizes. We measured only rms center-to-end distances of the arms (end-to-end distances for $f = 1$). This was done "on the fly"; i.e., we did not store each configuration and measure its properties in a second step of analysis. The reason is that an off-line analysis would have required very large files, and reading a configuration from disk or tape would have been not much faster than creating it from scratch. We neither measured shape parameters nor radii of gyration, since any such additional measurement would have slowed down the analysis considerably and since the main

Table 1. Main Results

f	N	runs	γ_f	previous estimates	A_f/A_1	previous estimates
1	8000	486×10^6	1.1573(2)	1.1575(6)[a]	1.0	
2	4000	71×10^6	1.1573		1.0614(5)	1.0628[f]
3	4000	83×10^6	1.0426(7)	1.089(1)[b]	1.1123(5)	1.1139;[f] 1.128[g]
4	4000	142×10^6	0.8355(10)	0.879(1)[b]	1.1553(6)	1.1581[f]
5	4000	114×10^6	0.5440(12)	0.567(2)[b]	1.1939(8)	
6	3000	73×10^6	0.1801(20)	0.16(1);[b] 0.14[c]	1.2295(9)	1.2322;[f] 1.265[g]
7	2500	73×10^6	−0.2520(25)	−0.33, −0.20[c]	1.2626(11)	
8	2300	59×10^6	−0.748(3)	−0.88, −0.60;[c] −1.00[d]	1.2934(12)	1.2951[f]
9	2150	48×10^6	−1.306(5)	−1.51, −1.01[c]	1.3225(14)	
10	2000	67×10^6	−1.922(7)		1.3494(16)	1.3519;[f] 1.424[g]
12	1700	73×10^6	−3.296(9)	−3.35;[d] −3.4(3)[e]	1.4014(17)	1.4017[f]
14	1400	66×10^6	−4.874(9)	−4.94[d]	1.4481(19)	
16	1200	96×10^6	−6.640(10)	−5.90[d]	1.4917(24)	
18	1100	96×10^6	−8.575(12)	−8.12;[d] −8.9(2)[e]	1.532(3)	
20	1000	130×10^6	−10.66(2)	−11.33[d]	1.574(4)	1.660[g]
24	800	147×10^6	−15.32(4)	−18.13[d]	1.643(5)	
30	500	316×10^6	−23.40(6)		1.735(7)	1.896[g]
40	300	880×10^6	−39.55(13)		1.883(14)	2.036[g]
50	120	1194×10^6	−59.2(2)		1.95(2)	2.208[g]
60	80	1712×10^6	−81.5(4)		2.04(3)	
70	61	1944×10^6	−108.0(7)		2.13(4)	
80	45	1966×10^6	−135.7(13)		2.16(6)	

[a] Reference 37, Monte Carlo. [b] Reference 16, Monte Carlo. [c] Reference 6, ϵ-expansion. [d] Reference 17, Monte Carlo. [e] Reference 19, Monte Carlo. [f] Reference 20, Monte Carlo (tetrahedral lattice). [g] Reference 22, molecular dynamics (off-lattice; values for $N = 50$).

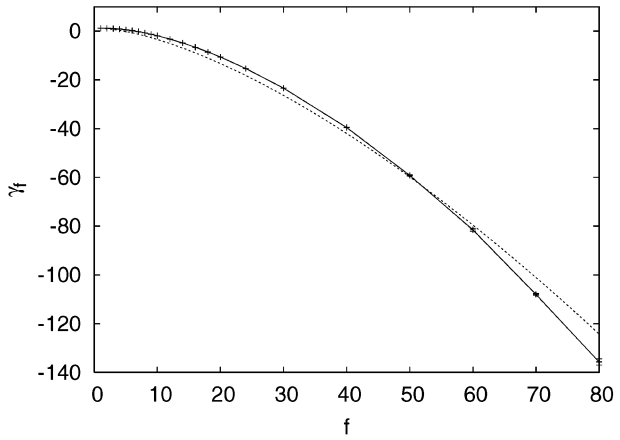

Figure 4. Exponents γ_f vs f. The full line is just a polygon connecting the points, and the dashed line is a fit with the large-f behavior as predicted by the cone approximation, eq 8.

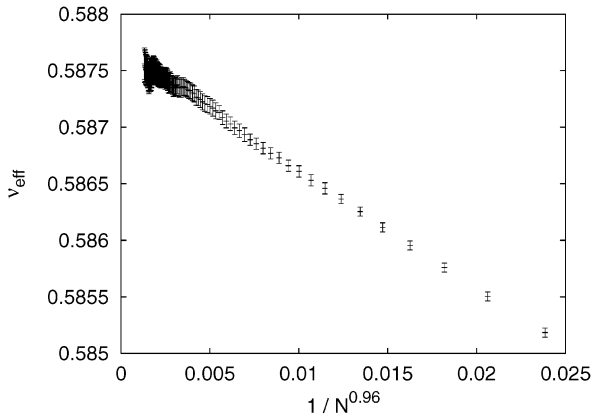

Figure 5. Effective exponents $\nu_{\text{eff}}(N)$ for linear "magical" Domb−Joyce polymers against $1/N^{0.96}$.

purpose of the present work was to demonstrate the efficiency of PERM and to study the main universal properties of large stars.

As for γ_f, we first need a careful analysis of linear chains to obtain precise estimates of ν and of the amplitude A_1. In Figure 5, we plot effective exponents $\nu_{\text{eff}}(N) = (\ln 16)^{-1} \ln[R^2_{8N}/R^2_N]$, again vs $1/N^{0.96}$. We see again a straight line (as in Figure 1), verifying again that the correction to scaling exponent is close to 1. Extrapolating to $N \to \infty$, we find $\nu = 0.58767(20)$. Together with previous estimates reviewed in ref 35, this gives our best estimate

$$\nu = 0.58765 \pm 0.00020 \tag{9}$$

Notice that this is more precise than the field theoretic estimates obtained from the ϵ-expansion.[4] The resulting amplitude is then

$$A_1 = \lim_{N\to\infty} R^2_N/N^{2\nu} = 0.8038 \pm 0.0005 \tag{10}$$

To obtain the amplitudes A_f for stars, we assume the value of ν as given above. We can then plot either $R^2_{N,f}/N^{2\nu}$ vs N (which gives A_f directly) or $R^2_{N,f}/R^2_N$ vs N, which gives A_f/A_1. To check for systematic corrections, we did both. Some typical curves obtained with the first method are shown in Figure 6. For each value of f we see two curves, one for each variant of the model: the upper curve is always that with the center f times occupied, and the lower one corresponds to a singly occupied center. For large values of f ($f \geq 40$) we see large fluctuations, indicating the limit where our sampling breaks down. Otherwise, we see large corrections to scaling, but they all are dominantly $\sim 1/N$, i.e., analytic corrections, and they have rather small influences on our final estimates of A_f.

These estimates are given in Table 1 and plotted in Figure 7. We show indeed the ratios A_f/A_1, to facilitate the comparison with previous estimates. The best previous estimates are those of Zifferer[20] and are also given in Table 1. We see very good agreement, even if most of the values of ref 20 are outside our error bars. The data of Zifferer were obtained from simulations on the tetrahedral lattice, and they indicate that the ratios A_f/A_1 are indeed universal. In ref 22, stars with up to 80 arms were simulated off-lattice by means of molecular dynamics. But it seems that the stars with $N = 100$ were not equilibrated, at least for $f = 1$ (see Table 1 of ref

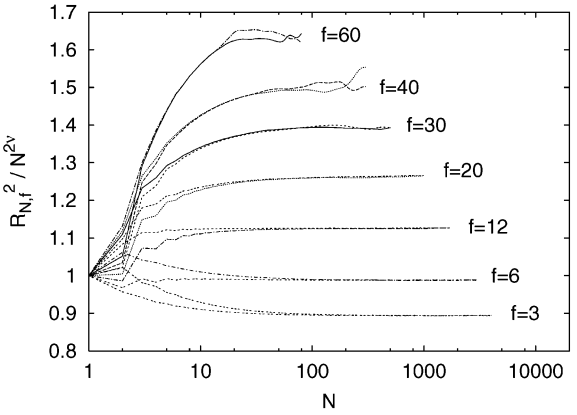

Figure 6. $R_{N,f}^2/N^{2\nu}$ plotted vs ln N, for seven selected values of f. For each f, results are shown for both variants of the model (single occupancy of the center: lower curve; f-fold occupancy: upper curve). The structures seen for $f \geq 40$ and large N are statistical fluctuations.

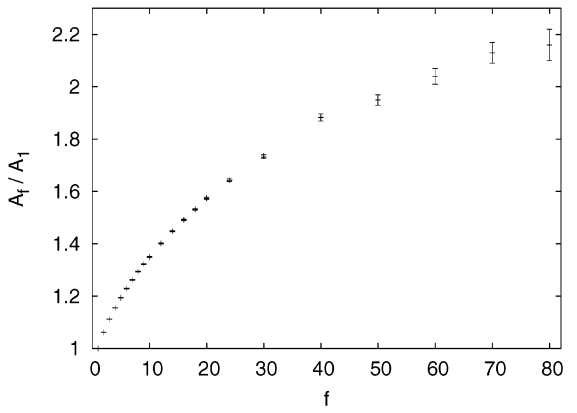

Figure 7. Amplitude ratios A_f/A_1 plotted against f.

22). Therefore, we list for comparison only the data for $N = 50$. They are systematically larger than our results and those of ref 20, and the discrepancy increases with f. This suggests that even these simulations had not reached equilibrium.

The most cited predictions for A_f/A_1 are from a heuristic blob model.[9,10] It gives

$$\frac{R_{N,f}^2}{R_N^2} \sim f^{1-\nu} \sim f^{0.41} \tag{11}$$

which is in gross violation with our data. The fact that this Daoud−Cotton model gives a too strong swelling with f is well-known.[20,40] Our data cannot be fitted by a pure power law, but asymptotically (for $f \to \infty$) they tend roughly to $A_f/A_1 \approx 0.78 f^{0.235}$. Again, we do not expect this to be the true asymptotic behavior, but it provides at least a useful guide for extrapolations.

Renormalization group (RG) calculations of star polymer sizes have been performed in refs 11 and 12, but it was already pointed out in refs 14 and 13 that these have difficulties in describing the large-f behavior. Using their own simulations to fix some of the parameters in an improved RG calculation, Lue and Kiselev[13,14] were able to fix these problems in the sense that their RG calculation described perfectly the behavior of the penetration function.[13,14] Unfortunately, they did not give predictions for A_f, so we cannot make a detailed comparison with our data. But we should point out that refs 13 and 14 also obtained much less swelling with f than predicted in refs 9, 11, and 12.

4. Discussion

We have demonstrated that chain growth methods with resampling, and the PERM algorithm in particular, are able to produce very precise Monte Carlo data for star polymers with many arms. Using the Domb−Joyce model on the simple cubic lattice, we combined this with absence of leading corrections to scaling and with the possibility to connect arbitrarily many arms to a point-like core. This allowed us to test conjectured scaling laws for the entropic critical exponents γ_f and for the f-dependent swelling of single arms. In principle, we could have measured during these simulations also other observables like monomer densities, star shapes, radii of gyration, etc.

Our most interesting results are for the exponents γ_f. All previous simulations were compatible with the predictions from the heuristic Daoud−Cotton model, but they were not very precise. There are also no good experimental results for these exponents, although they are fundamental for the entropy (and thus also for the free energy) of star polymers in good solvents. Our results show that these predictions are qualitatively correct (γ_f is negative and diverges as $-f^{\alpha}$, but the exponent α clearly disagrees with the prediction).

We also disagree with the prediction of the Daoud−Cotton model for the sizes of star polymers, and indeed the disagreement for the end-to-center distances is larger than for γ_f. They increase with f much slower than predicted. But this finding is not entirely new; it had been observed previously in Monte Carlo simulations.[20,40] Our data are compatible with these, but more precise and extending to larger values of f. Disagreement with the Daoud−Cotton prediction for star polymer sizes was also found in some experiments,[41] but there are also repeated claims in the literature[22,42] that experiments are compatible with it. We have no good explanation for the latter, except that the interpretation of experiments for diluted solutions might be less easy than anticipated.

With slight modifications of the algorithm one can also study related problems like stars center-absorbed to surfaces,[43] stars confined between two planar walls,[44] heterostars,[7,40] interactions between two star polymers,[13,38,45,46] or star polymer−colloid interactions.[47] We expect that PERM will be more efficient than previous algorithms (not the least because it gives immediately precise entropy estimates), in particular if applied to lattice models. PERM can also be applied off-lattice,[31,48] but its advantage is in general less pronounced there. We hope to present simulations for some of these problems in the near future.

References and Notes

(1) Grest, G. S.; Fetters, L. J.; Huang, J. S.; Richter, D. *Adv. Chem. Phys.* **1996**, *XCIV*, 67.
(2) Storey, R. F.; Nelson, M. E. *Appl. Polym. Sci.* **1997**, *66*, 151.
(3) de Gennes, P. G. *Scaling Concepts in Polymer Physics*; Cornell University Press: Ithaca, NY, 1979.
(4) des Cloizeaux, J.; Jannink, G. *Polymers in Solution*; Clarendon Press: Oxford, 1990.
(5) Duplantier, B. *Phys. Rev. Lett.* **1986**, *57*, 941.
(6) Schäfer, L.; von Ferber, C.; Lehr, U.; Duplantier, B. *Nucl. Phys. B* **1992**, *374*, 473.
(7) von Ferber, C.; Holovatch, Yu. *Phys. Rev. E* **2002**, *65*, 042801; *Condens. Matter Phys.* **2002**, *5*, 117.

(8) Zimm, B. H.; Stockmayer, W. H. *J. Chem. Phys.* **1949**, *17*, 1301.
(9) Daoud, M.; Cotton, J. P. *J. Phys. (Paris)* **1982**, *43*, 531.
(10) Birshtein, T. M.; Zhulina, E. B. *Polymer* **1984**, *25*, 1453.
(11) Miyake, A.; Freed, K. F. *Macromolecules* **1983**, *16*, 1228.
(12) Douglas, J. F.; Freed, K. F. *Macromolecules* **1984**, *17*, 1854.
(13) Lue L.; Kiselev, S. B. *Condens. Matter Phys.* **2002**, *5*, 73.
(14) Lue, L.; Kiselev, S. B. *J. Chem. Phys.* **2001**, *114*, 5026.
(15) Barrett, A. J.; Tremain, D. L. *Macromolecules* **1987**, *20*, 1687.
(16) Batoulis, J.; Kremer, K. *Macromolecules* **1989**, *22*, 4277.
(17) Shida, K.; Ohno, K.; Kimura, M.; Kawazoe, Y. *Macromolecules* **2000**, *33*, 7655.
(18) Di Cecca, A.; Freire, J. J. *Macromolecules* **2002**, *35*, 2851.
(19) Ohno, K. *Condens. Matter Phys.* **2002**, *5*, 15.
(20) Zifferer, G. *Macromol. Theory Simul.* **1999**, *8*, 433.
(21) Grest, G. S.; Kremer, K.; Witten, T. A. *Macromolecules* **1987**, *20*, 1376.
(22) Grest, G. S. *Macromolecules* **1994**, *27*, 3493.
(23) In principle, one could also use a modified pivot algorithm for measuring γ exponents,[37] but this has not yet been done for star polymers.
(24) Domb, C.; Joyce, G. S. *J. Phys. C* **1972**, *5*, 956.
(25) This implies that the density in the core region can become larger than one, which might seem unphysical. But the Domb−Joyce model is a coarse-grained model where the lattice constant can be understood to be much larger than the real monomer size. Densities larger than one do not present problems.
(26) Grassberger, P.; Sutter, P.; Schäfer, L. *J. Phys. A* **1997**, *30*, 7039.
(27) Belohorec, P.; Nickel, B. G. Accurate Universal and Two-Parameter Model Results from a Monte-Carlo Renormalization Group Study. Guelph University preprint, 1997.
(28) Lue, L.; Kiselev, S. B. *J. Chem. Phys.* **1999**, *111*, 5580.
(29) Baumgärtner, A. *J. Chem. Phys.* **1982**, *76*, 4275.
(30) Krüger, B.; Schäfer, L. *J. Phys. I* **1994**, *4*, 757; *Macromolecules* **1996**, *29*, 4737.
(31) Grassberger, P. *Phys. Rev. E* **1997**, *56*, 3682.
(32) Rosenbluth, M. N.; Rosenbluth, A. W. *J. Chem. Phys.* **1955**, *23*, 356.
(33) Frauenkron, H.; Causo, M. S.; Grassberger, P. *Phys. Rev. E* **1999**, *59*, R16.
(34) Hsu, H.-P.; Grassberger, P. *Eur. Phys. J. B* **2003**, *36*, 209; e-print cond-mat/0308276 2003.
(35) Hsu, H.-P.; Grassberger, P. *J. Chem. Phys.* **2004**, *120*, 2034; e-print cond-mat/0309314 2003.
(36) Causo, M. S.; Coluzzi, B.; Grassberger, P. *Phys. Rev. E* **2000**, *62*, 3958.
(37) Causo, M. S.; Caracciolo, S.; Pelissetto, *Phys. Rev. E* **1998**, *57*.
(38) Witten, T. A.; Pincus, P. A. *Macromolecules* **1986**, *19*, 2509.
(39) Ohno, K.; Binder, K. *J. Phys. (Paris)* **1988**, *49*, 1329.
(40) Havrankova, J.; Limpouchova, Z.; Prochazka, K. *Macromol. Theory Simul.* **2003**, *12*, 512.
(41) Held, D.; Müller, H. E. *Macromol. Symp.* **2000**, *157*, 225.
(42) Willner, L.; et al. *Macromolecules* **1994**, *27*, 3821.
(43) Shida, K.; Ohno, K.; Kimura, M.; Kawazoe, Y. *J. Chem. Phys.* **1996**, *105*, 8929.
(44) Romiszowski, P.; Sikorski, A. *J. Chem. Phys.* **2002**, *116*, 1731.
(45) Jusufi, A.; Watzlawek, M.; Löwen, H. *Macromolecules* **1999**, *32*, 4470.
(46) Rubio, A. M.; Freire, J. J. *Comput. Theor. Polym. Sci.* **2000**, *10*, 89.
(47) Jusufi, A.; Dzubiella, J.; Likos, C. N.; von Ferber, C.; Löwen, H. *J. Phys. C* **2001**, *13*, 6177.
(48) Hsu, H.-P.; Mehra, V.; Grassberger, P. *Phys. Rev. E* **2003**, *68*, 037703.

MA0355958